Sm- and Yb-induced reconstructions of the Si(111) surface

C. Wigren, J. N. Andersen, and R. Nyholm
Department of Synchrotron Radiation Research, Institute of Physics, Lund University, Sölvegatan 14, S-223 62 Lund, Sweden and MAX-lab, Lund University, Box 118, S-221 00 Lund, Sweden

M. Göthelid, M. Hammar, C. Törnevik, and U. O. Karlsson
Department of Physics, Material Science, Royal Institute of Technology, S-100 44 Stockholm, Sweden
(Received 1 March 1993)

Low-energy electron diffraction, scanning tunneling microscopy, and photoelectron spectroscopy results from the submonolayer Sm- and Yb-induced surface structures are presented. Several similar metal-induced surface reconstructions are found to exist for Yb and Sm on Si(111) for low submonolayer coverages: 3×2, 5×1, and 7×1. At higher submonolayer coverage, Yb induces a 2×1 reconstruction while Sm induces a $(\sqrt{3}\times\sqrt{3})R30°$-like reconstruction. Yb is found to be divalent in all structures, whereas the Sm valence increases with increasing coverage. In the 3×2 structure only divalent Sm is present, in the 5×1 and 7×1 structures a small amount of trivalent Sm appears, and, finally, in the $(\sqrt{3}\times\sqrt{3})R30°$ structure approximately half of the Sm atoms are trivalent. The surface Fermi-level position in the band gap for the different Sm and Yb reconstructions has been measured. The difference in valence stability between Sm and Yb is suggested to be the cause of the difference in the high-coverage structures found and the differences in pinning level for the two elements observed for the 5×1 and 7×1 structures.

INTRODUCTION

The valence changes of rare-earth atoms as they are placed in different chemical surroundings are a subject that has attracted much attention in recent years.[1] Part of this attention has been devoted to studies of monolayer coverage films of these elements on various substrates (see, e.g., Refs. 1–6). In several of these studies a change of the valence and thereby also of the number of $4f$ electrons of the rare-earth adsorbate has been found to occur as the coverage is changed (see, e.g., Refs. 5 and 6). In the present paper we report the results of an investigation of such submonolayer Sm and Yb films on Si(111). Whereas the valence change is a most interesting subject on its own, the emphasis of the paper is more directed towards how the difference in valence stability between Yb and Sm influences other properties of the surface such as, e.g., the Fermi-level pinning at the surface and the type of reconstructions that are formed. We would, for instance, expect a difference between the reconstructions formed by divalent and trivalent Sm, respectively. The reason for this expectation is that trivalent and divalent metals are known to induce different surface structures on Si(111).[7–13] This can to a large extent be attributed to their different number of valence electrons and to the fact that one of the main driving forces behind clean and metal-induced surface structures on Si(111) is dangling-bond elimination. When a trivalent metal is adsorbed on Si(111) all dangling bonds in a truncated bulk surface can be saturated if the metal atoms are adsorbed in the three-fold sites directly above the second- (the T_4 site) or the fourth- (the H_3 site) layer Si atoms at $\frac{1}{3}$ monolayer [1 ML=1 atom per Si(111) surface unit mesh] metal coverage in a $(\sqrt{3}\times\sqrt{3})R30°$ structure.[7–9] When divalent metals adsorb on the Si(111) substrate it might instead be natural to expect that the metal atoms adsorb in bridge sites which for $\frac{1}{2}$ ML would give a complete dangling-bond elimination in a 2×1 reconstruction. To investigate these matters we have used high-resolution core-level spectroscopy of the Si $2p$ and the rare-earth $4f$ levels, low-energy electron diffraction (LEED) to study the long-range order of the reconstructions, and finally scanning tunneling microscopy (STM) for investigating the more local bonding arrangements in the various structures.

EXPERIMENT

The photoelectron spectroscopy measurements were performed in two different ultrahigh vacuum (UHV) chambers at two different beamlines, a toroidal grating monochromator[14] and a plane grating monochromator[15] at the MAX-LAB synchrotron radiation facility. A double pass cylindrical mirror analyzer[14] or a hemispherical electron energy analyzer using a multichannel detection system[16] was used for the recording of the photoelectron spectra. The scanning tunneling microscopy (STM) measurements on the Sm/Si(111) system were performed at the Materials Science Department with a commercial instrument[17] in an UHV system including the STM and a preparation chamber. All chambers had a base pressure around or below $(1-2)\times10^{-10}$ torr. The samples were Si(111) wafers of n type, doped with Sb ($\rho=1-10\ \Omega$ cm). Most samples were cleaned and given thin oxide layers before insertion into the vacuum chamber.[18] The thin oxide layer was removed prior to use by heating in a vacuum below 10^{-9} torr. The surfaces were checked with

LEED and STM which revealed excellent 7×7 structures and photoelectron spectroscopy (PES) which showed characteristic surface-shifted components in the Si $2p$ spectra[19] and strong surface states in the valence-band region.[20] Contamination by C and O was also checked with PES of the O $1s$ and C $1s$ core levels. The amount of O was below the detection limit and only a small amount of C was seen. Sm and Yb were evaporated onto the clean Si(111) surfaces from a tantalum tube heated by radiation from a tungsten filament. During evaporation the pressure never rose above 9×10^{-10} torr [$(2-6)\times10^{-9}$ torr in the STM experiments]. Ordered surface reconstructions were obtained by annealing to around 500 °C after evaporating the appropriate amount onto the Si(111) substrate held at room temperature or by evaporating onto a warm substrate. A surface reconstruction could also always be obtained from a higher coverage by annealing to a higher temperature to desorb part of the Yb or Sm atoms.

RESULT AND DISCUSSION

At low and intermediate coverages Sm and Yb induce reconstructions with similar unit cells; it is only for the highest submonolayer coverage structure that the two elements give rise to different reconstructions. The series of similar reconstructions is as follows, in order of increasing coverage: 3×1 with half-order streaks [Fig. 1(a)], 5×1, and 7×1. (Note that we, for reasons discussed below, also use the designation 3×2 for the streaked 3×1 structure.) Following the 7×1 structure different reconstructions develop for Yb and Sm; a 2×1 pattern is formed for Yb whereas for Sm a pattern reminiscent of a $(\sqrt{3}\times\sqrt{3})R30°$ pattern develops. This LEED pattern is not a true $(\sqrt{3}\times\sqrt{3})R30°$ surface structure because of the presence of additional rather weak, large, and diffuse spots, not compatible with a $(\sqrt{3}\times\sqrt{3})R30°$ symmetry [Fig. 1(b)], but despite this for simplicity we use the designation $(\sqrt{3}\times\sqrt{3})R30°$. The 2×1 pattern formed by Yb is excellent with very sharp spots and a very low background. Without in any way being of poor quality the other $n\times1$ LEED patterns are not as excellent as this 2×1 pattern. The streaking observed in the 3×1 LEED patterns indicates that one-dimensional disorder exists in this surface structure. In an earlier investigation of the 3×1 Yb reconstruction[12] it was seen by STM that the true surface structure was actually a disordered 3×2 structure. The STM image in Fig. 2(a) of a Sm-induced streaked 3×1 surface demonstrates that this Sm-induced reconstruction behaves completely analogous. The surface structure consists of rows in one of the equivalent $\langle 1\bar{1}0\rangle$ directions with adjacent rows being separated by $3a$ [$a=3.84$ Å is the characteristic unit distance in the Si(111) surface] and with protrusions separated by $2a$ along the rows leading to a local 3×2 structure. The phase of the $\times2$ order along the rows is, however, more or less random for adjacent rows which results in half-order streaks instead of dots in the LEED pattern.[12] We will therefore designate this structure 3×2 instead of streaked 3×1.

An interesting feature of the rare-earth atoms is the quite small energy separation between the divalent and the trivalent state, where in the latter state an extra $4f$ core electron has been promoted to the valence band. Because of this property the valence of a rare-earth atom, and therefore also its number of $4f$ core electrons, depends on its chemical surroundings. Thus $4f$ core-level spectra, which appear very differently for divalent and trivalent rare earths,[21] may be used for assessing the valence. From the Sm and Yb $4f$ spectra[22] in Fig. 3 it is directly seen that both of these rare-earth elements are divalent in the case of the 3×2 reconstruction. This valence state and the semiconducting properties of the reconstructions seen from the lack of emission at the Fermi level in Fig. 3 are consistent with the even number of Si atoms in a 3×2 unit cell but would have been inconsistent with the odd number of Si atoms in a 3×1 unit cell. Comparing now the Si $2p$ spectra from the two 3×2 surfaces, Fig. 4, it is seen that they are almost identical. This similarity of the Si $2p$ spectra and of the STM pictures makes us conclude that the local bonding structure of the Sm 3×2 surface is the same as found for the Yb 3×2 structure,[12] that is, the Sm atoms adsorb in bridge positions on the Si(111) surface. Finally it should be not-

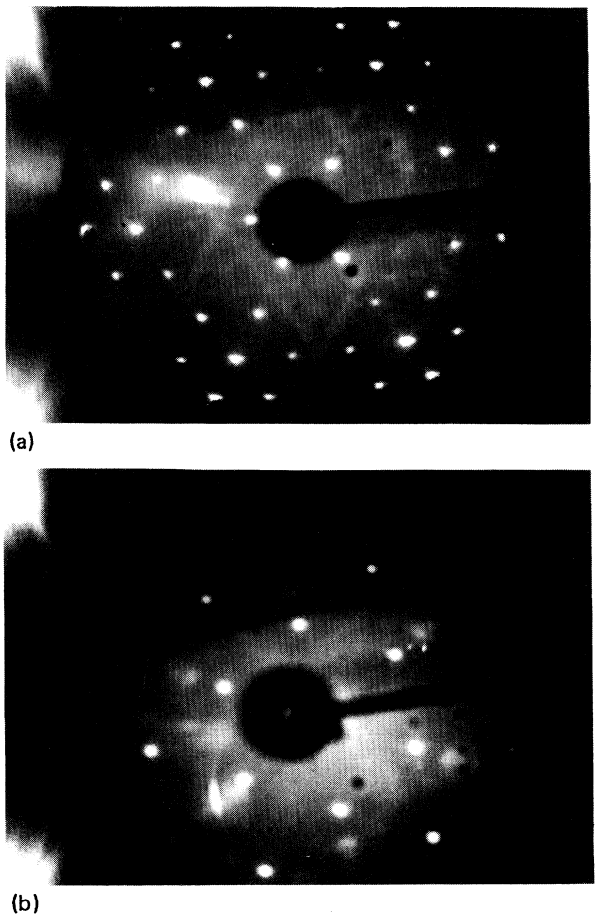

FIG. 1. LEED patterns from the submonolayer Sm-induced 3×2 (a) and $(\sqrt{3}\times\sqrt{3})R30°$ (b) surface structures. Note that the pattern displayed in (b) is not a true $(\sqrt{3}\times\sqrt{3})R30°$ pattern.

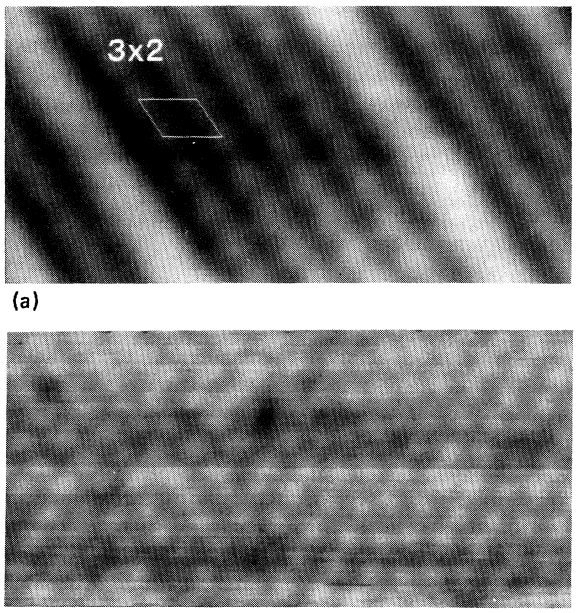

FIG. 2. STM images from the Sm-induced 3×2 (a) and $(\sqrt{3}\times\sqrt{3})R30°$ (b) surface structures.

ed that the close resemblance of the Si $2p$ spectra for the Yb- and Sm-induced 3×2 structures means that also the Sm structure contains the shifted component due to emission from the second Si layer found for the Yb 3×2 structure.[12] The general conclusion concerning the Sm and Yb 3×2 structures, that they are very similar in all respects, is not surprising given the well-known similar

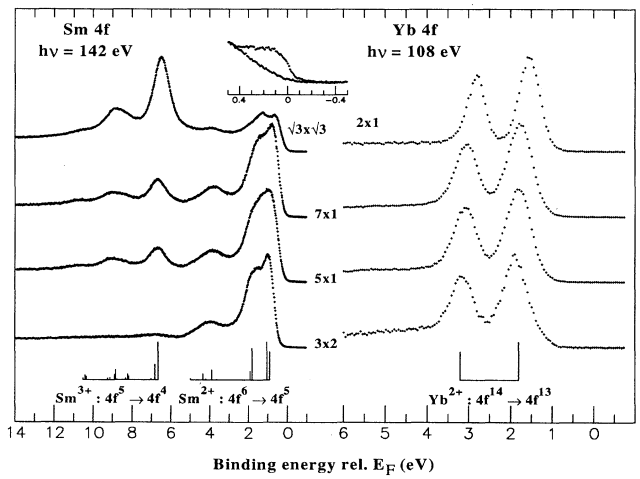

FIG. 3. Sm and Yb $4f$ spectra from the different submonolayer metal-induced surface reconstructions. The theoretical multiplet patterns for Sm are taken from Ref. 21. Spectra recorded at a photon energy of 40 eV from the Sm-induced $(\sqrt{3}\times\sqrt{3})R30°$ structure and from a metallic Ta foil are shown in the inset. Note the lack of intensity at the Fermi level in the spectrum from the $(\sqrt{3}\times\sqrt{3})R30°$ structure.

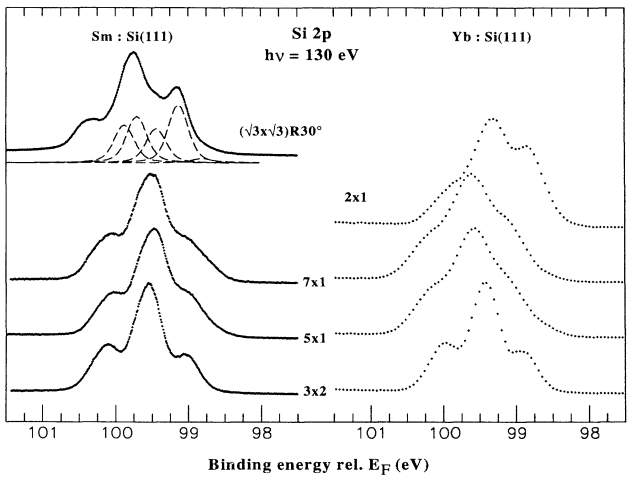

FIG. 4. Si $2p$ spectra from the different Sm- and Yb-induced surface structures on Si(111). The spectrum from the $(\sqrt{3}\times\sqrt{3})R30°$ structure has been fitted with five spin-orbit-split components. The full line shows the result of the fit and the dashed lines show the individual $2p_{3/2}$ components.

chemical behavior of rare-earth atoms of the same valence.

The STM image in Fig. 2(a) in addition to the 3×2 structure also shows some broader stripes oriented along the $\langle 1\bar{1}0\rangle$ directions. These stripes are characteristic of the 5×1 reconstructions for Sm and Yb. STM pictures taken at higher resolution reveal that these stripes actually consist of two parallel rows separated by a distance of $2a$. It is difficult to resolve any clear structure along the rows, and we therefore assign a $\times1$ periodicity in this direction. The 5×1 periodicity is created by an arrangement of such parallel *double* rows on the surface with a distance of $3a$ separating them. This can of course also be described as an arrangement of *single* rows with a distance that alternates between $2a$ and $3a$. The 7×1 structure is conveniently described in the same picture as consisting of single rows whose distance repeats in a $2a,2a,3a$ pattern. Noteworthy is that the 5×1 and 7×1 structures appear to be of the same type in the Yb/Si(111) and Sm/Si(111) systems. In the case of Yb this pattern of development with fewer and fewer rows separated by $3a$ continues also for coverages above that of the 7×1 reconstruction eventually resulting in a 2×1 structure where all of the rows are separated by $2a$.[12] In the case of Sm a structure of a type completely different from the earlier $n\times1$ structures is formed at higher coverages than the 7×1. We will return to this Sm structure and describe it in more detail later.

From the Yb $4f$ spectra, Fig. 3, we find that all of the $n\times1$ Yb structures involve only divalent Yb. The lack of emission at the Fermi level observed in Fig. 3 shows that all of these reconstructions are semiconducting. In the case of Sm this semiconducting property is not so clearly seen in the spectra, Fig. 3, simply because of the lower binding energy of the divalent Sm $4f$ peaks, however we would still argue that these structures are semiconducting. This is supported by a more detailed inspection of

spectra from the valence band where no intensity is found at the Fermi level in the $(\sqrt{3}\times\sqrt{3})R30°$ structure [see the inset in Fig. 3 where spectra, recorded with a photon energy of 40 eV, from the Sm-induced $(\sqrt{3}\times\sqrt{3})R30°$ structure and from a metallic Ta foil are compared]. Concerning the Sm valence a trivalent $4f$ Sm signal is seen in the binding-energy range from 5 to 12 eV. The trivalent intensity in the 5×1 and 7×1 surfaces may from off-resonance spectra, recorded with a photon energy of 200 eV, be estimated to be roughly 10–20 % of the divalent signal. These observations concerning the valence and the nonmetallic nature of the 5×1 and the 7×1 surfaces are not compatible with the simple model suggested from the STM pictures. If the rows of that model are placed on a truncated Si(111) surface and are assumed to consist of divalent Sm or Yb atoms, the surface will be metallic because of the odd number of electrons in one unit cell. In the case of Sm it could be argued that some of the Sm atoms actually become trivalent so as to achieve an even number of electrons in the unit cell. However, if the mixed valence in these structures is of heterogeneous type, i.e., due to two different Sm sites where the Sm atoms are divalent and trivalent, respectively, then there has to be at least five Sm atoms per unit cell with only one of them being trivalent. This is clearly inconsistent with the interpretations in terms of $n\times1$ unit cells. The other possible explanation, namely, that the mixed valency is of homogeneous type, i.e., that the Sm atoms flip between being divalent and trivalent (which could yield any mean valence between 2 and 3), does not seem obvious to us in a system that is not metallic.[23] We are not aware of any other semiconducting system where such homogeneous mixed valence has been shown to exist. This results in the realization that the 5×1 and 7×1 reconstructions are quite complicated structures involving a reconstruction of (at least) the outermost Si(111) layer. Similar testimony for the nonsimple nature of these reconstructions is provided by Si $2p$ spectra as discussed below. The solution to the problems could be that there is actually a $\times2$ periodicity along the rows. Such a periodicity could, for instance, be created by dimer formation in the single rows of Si atoms not bonding to Yb or Sm, however this has not been verified by STM. It is questionable if such a $\times2$ periodicity would be visible in LEED. First, Si is a much weaker scatterer of low-energy electrons than Yb or Sm, and second, the phase of this $\times2$ periodicity between different Si rows is most likely random simply because of the large distance between the rows which would lead to streaks instead of spots in the LEED pattern.

The Si $2p$ spectrum from the Yb-induced 2×1 reconstruction contains the same shifted components as found in the 3×2 structure. Based on this it was argued elsewhere[12] that the Yb site in the 2×1 structure is the same as in the 3×2 structure, that is, the Yb atoms adsorb in bridge positions. It might be expected that the same conclusion would be true for the 5×1 and the 7×1 structures also and that Si $2p$ spectra from these surfaces would consist of the same shifted components as found in the 3×2 structure. This is, however, not the case; a component with a significantly larger shift than any found in the 3×2 is present for both the 5×1 and the 7×1. This may be seen as a small shoulder on the low-binding-energy side of the spectra from the 5×1 and 7×1 structures in Fig. 4 although it is slightly obscured by the different Fermi-level pinning positions of the spectra. However, a direct comparison with shifted spectra (i.e., compensated for the difference in Fermi-level pinning positions) from the 3×2 or 2×1 structures or fittings (Fig. 5) of the spectra clearly reveals the existence of this component. The large shift (−0.8 eV) could be taken to indicate that it is due to Si atoms with a larger coordination to the rare-earth atoms than any Si atoms of the 3×2 structure. An alternative interpretation of this −0.8-eV shifted component would be to assign it to half of the dimer atoms that are proposed above to create a $\times2$ periodicity along the rows. Such dimerization is excluded in the 2×1 structure giving a natural exlanation as to why this component is not found in that structure. However, dimerization is possible in the 3×2 structure somewhat contradicting that the −0.8-eV component is not found in that structure. It was actually argued that such dimers were present and gave intensity to a component shifted by −0.5 eV in the 3×2 structure.[12] The additional −0.3-eV shift of the dimer atoms needed to give a total shift of −0.8 eV may, however, possibly be attributed to the different surroundings of the dimers in the 3×2 and the 5×1 or 7×1 (actually 5×2 or 7×2 in this interpretation) structures. Finally we note that, even though the Sm-induced structures contain small amounts of trivalent Sm while the Yb-induced structures only contain divalent Yb, the Si $2p$ spectra for Sm- and Yb-induced 5×1 and 7×1 surface structures are very similar, thus we would also expect that the usual geometrical

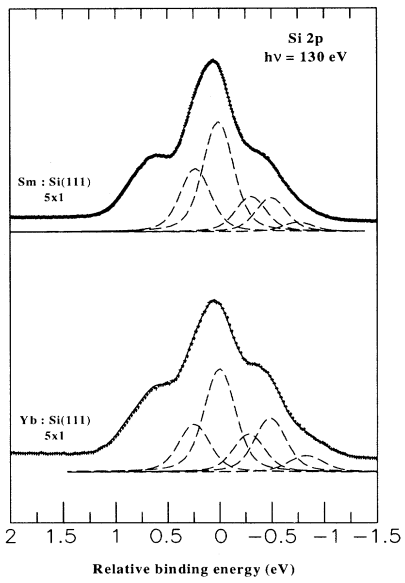

FIG. 5. Curve fittings of the Si $2p$ spectra (crosses) from 5×1 structures induced by Sm and Yb. The dashed lines show the individual $2p_{3/2}$ components and the full line the total fit. Binding energy is given relative the bulk Si $2p_{3/2}$.

structures are very alike. However, the apparent complexity of these reconstructions does not permit a more detailed discussion of the atomic structures than performed above.

In the case of Sm the submonolayer reconstruction with the highest coverage cannot be seen as a natural extension of an $n\times1$ structure. Instead of a 2×1 structure as for Yb, a $(\sqrt{3}\times\sqrt{3})R30°$ LEED pattern develops. As already remarked, this pattern in addition to the $\sqrt{3}$ spots contains extra diffuse spots indicating a distortion from a true $(\sqrt{3}\times\sqrt{3})R30°$ structure. A STM image from this reconstruction is shown in Fig. 2(b). The distance between adjacent protrusions is approximately 10 Å, which is not compatible with a $(\sqrt{3}\times\sqrt{3})R30°$ structure. Instead the structure seen in the image is probably connected to the spots seen in addition to the $(\sqrt{3}\times\sqrt{3})R30°$ spots in LEED. A further impression from the STM image is that the surface is rather disordered, which can explain the large sizes of these additional LEED spots. The Sm $4f$ spectra from this reconstruction, Fig. 3, show a much larger trivalent intensity than for any other of the mixed valent Sm overlayers. From spectra measured off-resonance the intensity ratio between divalent and trivalent Sm is found to be slightly below 1:1, i.e., there is most likely equal numbers of divalent and trivalent atoms in this structure. Presumably it is the lower energy required for Sm as opposed to Yb to promote a $4f$ electron and thereby make the atoms trivalent which is the cause of the different reconstructions chosen by these two rare earths at the highest submonolayer coverage.

The Sm-induced $(\sqrt{3}\times\sqrt{3})R30°$ structure is very complex as can be seen by the disorder observed in the STM images and by the number of components found in Si $2p$ spectra from this structure. To fit $2p$ spectra from the Sm-induced $(\sqrt{3}\times\sqrt{3})R30°$ surface requires at least five components (Fig. 4), which indicates that there is a large number of different Si sites in this structure. The complexity of the structure thus prohibits us from constructing a model of the $(\sqrt{3}\times\sqrt{3})R30°$ structure based on our data. However, our data reduce the number of possibilities for such a model. LEED shows two types of structures [the $(\sqrt{3}\times\sqrt{3})R30°$ structure and the structure due to the additional spots] while STM only shows a structure that probably causes the additional spots in LEED. This strongly indicates that the $(\sqrt{3}\times\sqrt{3})R30°$ structure consists of more than one layer, which is also consistent with the large number of components seen in the Si $2p$ spectra. The divalent and trivalent signal seen in the Sm $4f$ spectra in combination with these results further suggest that a model of the $(\sqrt{3}\times\sqrt{3})R30°$ structure should contain trivalent Sm in layers below the surface while the top surface layer should contain divalent Sm atoms with a rather poor long-range order.

We have already noted that although many surface structures for Yb and Sm on Si(111) are similar, a difference exists in valency for the Yb and Sm atoms. A further difference is the Fermi-level pinning position. The Fermi-level position in the Si band gap at the surface can be determined from bulk sensitive Si $2p$ spectra. This is done by measuring the binding energy of the Si substrate $2p$ component in the different surfaces as this binding energy is directly related to the Fermi-level position in the band gap. Since the Fermi level is known for the clean Si(111)7×7 surface[24] the binding energy of the substrate component for this surface reconstruction can be used as a reference. The Fermi-level positions in the band gap for the different submonolayer Yb- and Sm-induced surface structures are tabulated in Table I.

TABLE I. The Fermi-level position in the band gap relative to the valence-band maximum.

	Fermi-level position (eV)	
Surface	Yb	Sm
3×2	0.73	0.73
5×1	0.84	0.67
7×1	0.89	0.67
2×1	0.60	
$(\sqrt{3}\times\sqrt{3})R30°$		0.92

The trends of Table I may actually also be seen directly from the binding energy of the Si $2p$ components in the surface sensitive spectra in Fig. 4. The Fermi-level position is the same in the two 3×2 surfaces as would be expected from the similarity of these structures. The binding energy of the Si $2p$ components is slightly lowered in the spectra from the Sm-induced 5×1 and 7×1 surfaces which means that the Fermi-level position in the band gap is also slightly lowered. In the Yb-induced 5×1 and 7×1 surfaces the Fermi level moves towards the conduction-band minimum as compared to the 3×2 position. Since LEED, STM, and Si $2p$ spectra indicate that the Yb- and Sm-induced structures are very similar, the most probable explanation for the different Fermi-level position in the Yb- and Sm-induced 5×1 and 7×1 surfaces is that it is caused by the trivalent Sm present in these structures. In the 2×1 Yb-induced surface the Fermi-level position shifts to a position close to the middle of the band gap while the $(\sqrt{3}\times\sqrt{3})R30°$ Sm-induced structure has a Fermi-level position close to the conduction-band minimum. This position for Sm close to the conduction band is actually the position expected for trivalent epitaxial rare-earth silicides on Si(111).[25]

SUMMARY

Yb and Sm show a number of common submonolayer surface reconstructions when they are deposited on the Si(111) surface and annealed; these reconstructions are 3×2, 5×1, and 7×1. In addition, Yb shows a 2×1 and Sm a $(\sqrt{3}\times\sqrt{3})R30°$ reconstruction. The 3×2 structures for the two rare earths are shown to be very alike with respect to the adsorption site, which for Yb has been determined as a bridge position, and with respect to the pinning position of the Fermi level. In geometrical respects the 5×1 and 7×1 structures seem very similar for the two metals, however for Sm a weak trivalent signal is found for both of these structures whereas Yb is completely divalent. It was argued that the difference in the Fermi-level pinning position between the two ele-

ments was a consequence of this difference in valency. The different reconstructions at the highest-coverage structure were also argued to stem from the fact that part of the Sm atoms are trivalent whereas Yb still stays completely divalent.

ACKNOWLEDGMENTS

The authors acknowledge financial support from the Swedish Natural Science Research Council and the K. & A. Wallenberg Foundation.

[1]See, e.g., B. Johansson and N. Mårtensson, in *Handbook on the Physics and Chemistry of Rare Earths,* edited by K. A. Gschneidner, Jr., L. Eyring, and S. Hüfner (North-Holland, Amsterdam, 1987), Vol. 10.

[2]A. Franciosi, P. Perfetti, A. D. Katnani, J. H. Weaver, and G. Margaritondo, Phys. Rev. B **29**, 5611 (1984).

[3]Å Fäldt and H. P. Myers, Phys. Rev. B **33**, 1424 (1986); Solid State Commun. **48**, 253 (1983); Phys. Rev. Lett. **52**, 1315 (1984); Phys. Rev. B **30**, 5481 (1984).

[4]M. Grioni, J. J. Joyce, and J. H. Weaver, Phys. Rev. B **32**, 962 (1985).

[5]A. Nilsson, B. Eriksson, N. Mårtensson, J. N. Andersen, and J. Onsgaard, Phys. Rev. B **38**, 10 357 (1988).

[6]A. Stenborg, O. Björneholm, A. Nilsson, N. Mårtensson, J. N. Andersen, and C. Wigren, Phys. Rev. B **40**, 5916 (1989).

[7]M. Otsuka and T. Ichikawa, Jpn. J. Appl. Phys. **24**, 1103 (1985).

[8]J. Nogami, Sang-il Park, and C. F. Quate, J. Vac. Sci. Technol. B **6**, 1479 (1988).

[9]R. J. Hamers, Phys. Rev. B **40**, 1657 (1989).

[10]J. Kofoed, I. Chorkendorff, and J. Onsgaard, Solid State Commun. **52**, 283 (1984).

[11]The Ca/Si(111) system shows a 3×1, 5×1, and 2×1 surface reconstruction [J. F. Morar (private communication)].

[12]C. Wigren, J. N. Andersen, R. Nyholm, U. O. Karlsson, J. Nogami, A. A. Baski, and C. F. Quate, Phys. Rev. B **47**, 9663 (1993).

[13]W. A. Henle, M. G. Ramsey, F. P. Netzer, and K. Horn, Surf. Sci. **254**, 182 (1991).

[14]U. O. Karlsson, J. N. Andersen, K. Hansen, and R. Nyholm, Nucl. Instrum Methods Phys. Res. A **282**, 553 (1989).

[15]R. Nyholm, S. Svensson, J. Nordgren, and A. Flodström, Nucl. Instrum. Methods Phys. Res. A **246**, 267 (1986).

[16]J. N. Andersen, O. Björneholm, A. Sandell, R. Nyholm, J. Forsell, L. Thånell, A. Nilsson, and N. Mårtensson, Synch. Rad. News **4** (4), 15 (1991).

[17]Omicron Vakuum Physik GmbH, Taunusstein, Germany.

[18]A. Ishizaka and Y. Shiraki, J. Electrochem. Soc. **133**, 666 (1986).

[19]F. J. Himpsel, P. Heimann, T.-C. Chiang, and D. E. Eastman, Phys. Rev. Lett. **45**, 1112 (1980).

[20]F. J. Himpsel, D. E. Eastman, P. Heimann, B. Reihl, C. W. White, and D. M. Zehner, Phys. Rev. B **24**, 1120 (1981); T. Yokotsuka, S. Kono, S. Suzuki, and T. Sagawa, Solid State Commun. **39**, 1001 (1981).

[21]F. Gerken, J. Phys. F **13**, 703 (1983).

[22]We use a photon energy of 142 eV in the case of Sm to resonantly enhance the Sm $4f$ emission [J. W. Allen, L. I. Johansson, I. Lindau, and S. B. Hagstrom, Phys. Rev. B **21**, 1335 (1980)].

[23]If the mixed valence was of a homogeneous type the mean valency might be dependent on the temperature. We have performed measurements at different temperatures without seeing any changes in the valence.

[24]The Fermi-level pinning position for the clean Si(111)7×7 surface is 0.63 eV above the valence-band maximum; F. J. Himpsel, G. Hollinger, and R. A. Pollak, Phys. Rev. B **28**, 7104 (1983).

[25]J. Y. Duboz, P. A. Badoz, F. Arnaud d'Avitaya, and J. A. Chroboczek, Appl. Phys. Lett. **55**, 84 (1989).

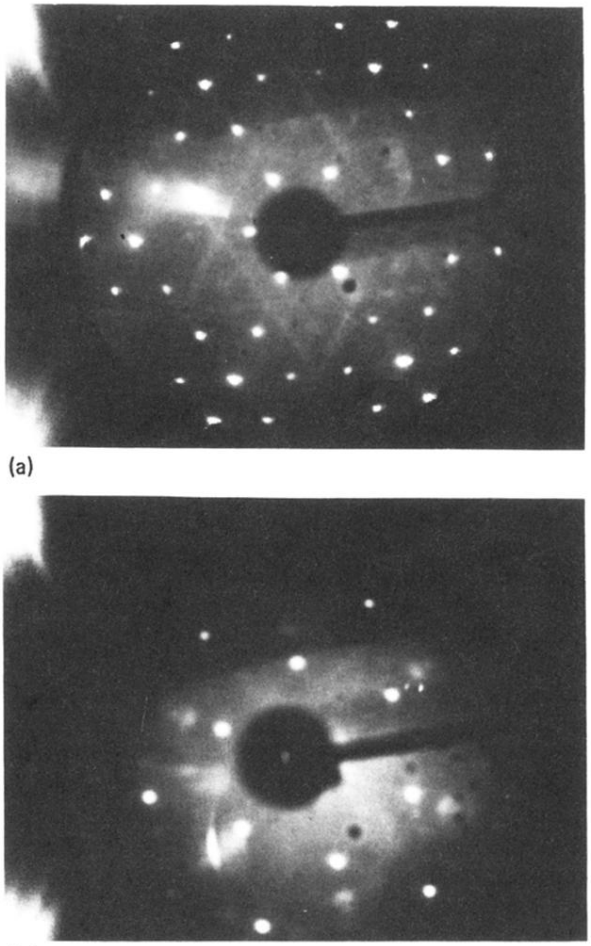

(a)

(b)

FIG. 1. LEED patterns from the submonolayer Sm-induced 3×2 (a) and $(\sqrt{3}\times\sqrt{3})R30°$ (b) surface structures. Note that the pattern displayed in (b) is not a true $(\sqrt{3}\times\sqrt{3})R30°$ pattern.

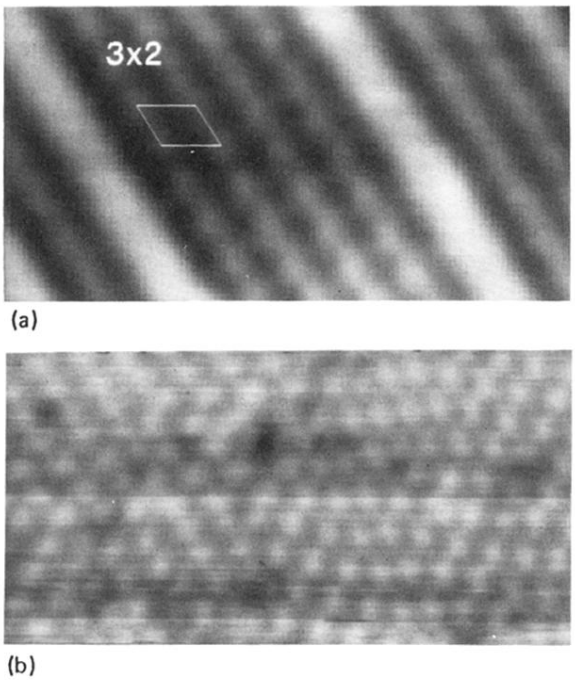

FIG. 2. STM images from the Sm-induced 3×2 (a) and $(\sqrt{3}\times\sqrt{3})R\,30°$ (b) surface structures.